

# New ligand bearing preorganized binding side-arms interacting with ammonium cations: Synthesis, conformational studies and crystal structure†‡

Mauro Formica,<sup>a</sup> Vieri Fusi,<sup>\*a</sup> Luca Giorgi,<sup>a</sup> Annalisa Guerri,<sup>b</sup> Simone Lucarini,<sup>c</sup> Mauro Micheloni,<sup>\*a</sup> Paola Paoli,<sup>b</sup> Roberto Pontellini,<sup>a</sup> Patrizia Rossi,<sup>b</sup> Giorgio Tarzia<sup>c</sup> and Giovanni Zappia<sup>\*c</sup>

<sup>a</sup> Institute of Chemical Sciences, University of Urbino, Piazza Rinascimento 6, I-61029, Urbino, Italy

<sup>b</sup> Department of Energy Engineering 'Sergio Stecco', University of Florence, Via S. Marta 3, I-50139, Florence, Italy

<sup>c</sup> Institute of Pharmaceutical Chemistry, University of Urbino, Piazza Rinascimento 6, I-61029, Urbino, Italy. E-mail: vieri@chim.uniurb.it

Received (in London, UK) 13th June 2003, Accepted 12th August 2003

First published as an Advance Article on the web 3rd September 2003

The synthesis and characterization of the new tetraazamacrocyclic 4-(N),10-(N)-bis[2-(3-hydroxy-2-oxo-2H-pyridin-1-yl)acetamido]-1,7-dimethyl-1,4,7,10-tetraazacyclododecane (**L**) is reported. **L** shows two 3-(hydroxy)-1-(carbonylmethylen)-2(1H)-pyridinone moieties as side-arms of a tetra-aza-macrocyclic base. The key coupling of side-arms was studied and the most significant results were obtained by activating the 3-(benzyloxy)-1-(carboxymethyl)-2(1H)-pyridinone as pentafluorophenol ester. The acid–base properties of **L** and its capability to interact with simple ammonium cations were investigated by potentiometric measurements in aqueous solution (298.1 ± 0.1 K, *I* = 0.15 mol dm<sup>-3</sup>). Protonated species of **L** can bind NH<sub>4</sub><sup>+</sup> or primary ammonium cations such as MeNH<sub>3</sub><sup>+</sup> discriminating them from secondary or tertiary ammonium cations such as Me<sub>2</sub>NH<sub>2</sub><sup>+</sup> or Me<sub>3</sub>NH<sup>+</sup> which are not bound in aqueous solution.

<sup>1</sup>H and <sup>13</sup>C NMR spectra showed the existence in solution of two conformers on the NMR time scale due to the rotational restriction of the two N–C=O groups. The activation parameters were determined by dynamic variable-temperature NMR analysis.

Molecular dynamics calculations gave results in agreement with the experimental data for both conformation and ammonium-binding studies, underlining that the transformation of the two secondary amines of the macrocyclic base to amide functions, forces the side-arms to remain fixed in position, almost face to face and thus to be preorganized to interact with other species. The crystal structure of the [HL]Cl·8H<sub>2</sub>O species shows the high number of preorganized hydrogen bond sites capable, in this case, of interacting directly with five H<sub>2</sub>O molecules.

## Introduction

Macrocyclic compounds are continuing to attract the interest of researchers in coordination chemistry. Indeed, the countless possible applications of these molecules, as well as their usefulness in fundamental studies, have made this a thriving field of study.<sup>1–5</sup> These ligands are used as selective binders of metal ions, simple models for biologically relevant systems, hosts for guests of various nature, catalysts, NMR contrast agents, photochemical devices, selective extractants, analytical reagents, *etc.*<sup>6–8</sup> A synthetic strategy to widen the potential applications of macrocycles is to use them as a base on which to attach suitable side-arms. In this way it is possible to combine different chemical properties, exploiting the characteristics of the molecular fragments connected as side-arms.<sup>9–11</sup> The attached moieties can also be driven to cooperate by the

macrocyclic skeleton, thus forming new binding sites inside the molecule having different hard–soft capabilities.<sup>12</sup>

3-Hydroxy-2(1H)-pyridinone and its derivative molecules are chelating agents that have shown particular binding and sequestering properties towards highly charged metal cations.<sup>13</sup> For example, they can produce decorporation of heavy metals in animals,<sup>14</sup> showing high affinity towards iron(III).<sup>15</sup> Moreover, this group shows several atoms able to form hydrogen bonds with other species.<sup>16</sup> This capability can be pH-modulated in solution, producing donors or acceptors of hydrogen bond sites.<sup>15c</sup> These moieties have usually been attached to linear scaffolds in the 4-position by an amide group; in the present study we used the 1,7-dimethyl-1,4,7,10-tetraazacyclododecane as macrocyclic base upon which we attached two 3-hydroxy-2(1H)-pyridinone molecules linked in the 1-position to the macrocycle with a methylene-carbonyl chain, obtaining the ligand **L** (Chart 1). The synthetic aspects were investigated and new ways of attaching the side-arm explored. In the final ligand **L**, the two secondary amines of the macrocyclic base were transformed into amide groups. In this way, these two functions play a fundamental role in pre-organizing the side-arms for the interaction with other species.

† Electronic supplementary information (ESI) available: molecular modeling studies. See <http://www.rsc.org/suppdata/nj/b3/b306778e/>

‡ Dedicated to Professor Paolo Dapporto, a great teacher and friend, on his 60th birthday.

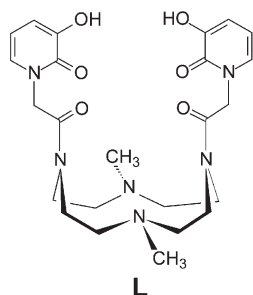


Chart 1 Ligand L.

The guests considered in this work are  $\text{NH}_4^+$ ,  $\text{MeNH}_3^+$ ,  $\text{Me}_2\text{NH}_2^+$  and  $\text{Me}_3\text{NH}^+$ , which could interact with the multiple hydrogen bonding sites of **L**. These guests were chosen considering that the recognition of ammonium and alkyl ammonium ions is of fundamental importance and practical interest, mainly in the biological fields.<sup>17</sup> For example, nonactin, a naturally occurring antibiotic that tightly binds  $\text{NH}_4^+$ , is used in commercial ion selective electrodes for detecting the cation in biological samples.<sup>18</sup> The binding capabilities of **L** toward such guests were investigated in aqueous solution and by molecular modeling. The synthesis of the ligand is reported together with its acid–base properties in aqueous solution. The crystal structure of the monoprotonated species  $\text{HL}^+$  and the location of the acidic protons in the several protonated species are presented.

## Results and discussion

### Synthesis

Scheme 1 outlines the synthesis of the new multidentate ligand **L**, which was based on the coupling of the protected acid **3** with the 1,7-dimethyl-1,4,7,10-tetraazacyclododecane **5**,<sup>19</sup> followed by the removal of the hydroxyl function protection.

The 3-(benzyloxy)-1-(carboxymethyl)-2(1*H*)-pyridinone **3** (Scheme 1) was prepared from the commercially available 2,3-dihydroxypyridine **1** in 71% yield following the method of Taylor *et al.*<sup>20,21</sup> with minor modifications. The key coupling step was studied in detail employing different coupling reagents, and the most significant results are reported in Table 1. Initial attempts to achieve coupling between the above acid **3**, as the corresponding succinimide derivative,<sup>20</sup> and the tetraamine **5** gave the bis-acetylated product **6** in moderate yields (45%, entry 1, Table 1).

Poor yields were obtained with coupling reagents such as DCCI (*N,N'*-dicyclohexylcarbodiimide),<sup>22</sup> *t*-BuCOCl

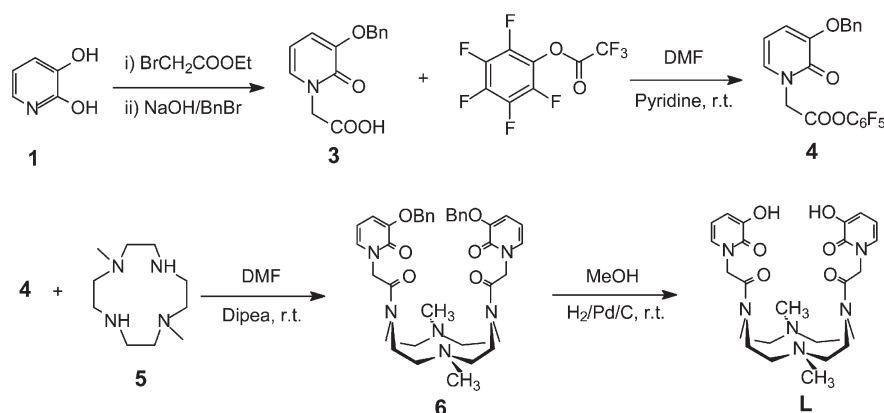
**Table 1** Coupling reagents for the activation of the carboxylic group function of **3** to give **6**

Entry	Coupling Reagent	Isolated Yield (%)
1	<i>N</i> -Hydroxysuccinimide/DCCI	45
2	DCCI	< 5
3	DMT-MM	< 5
4	<i>t</i> -BuCOCl/ $\text{Et}_3\text{N}$	< 5
5	EDCI/HOBT	10
6	EEDQ	51
7	2-Chloro-1-methyl pyridinium iodide/ $\text{Et}_3\text{N}$	51
8	<i>p</i> - $\text{NO}_2\text{C}_6\text{H}_4\text{OH}$ /DCCI	68
9	$(\text{Py})_2\text{S}_2/\text{PPh}_3$	78
10	$\text{CF}_3\text{COOC}_6\text{F}_5/\text{Py}$	87

(2,2-dimethylpropanoyl chloride)/ $\text{Et}_3\text{N}$ ,<sup>23</sup> DMT-MM (4-(4,6-dimethoxy-1,3,5-thiazin-2-yl)-4-methylmorpholinium chloride)/NMM (*N*-methylmorpholine),<sup>24</sup> and EDCI (*N*-(3-dimethylaminopropyl)-*N'*-ethylcarbodiimide)/HOBT (1-hydroxybenzotriazole)<sup>25</sup> (entries 2–5), whereas the use of EEDQ (2-ethoxy-1-ethoxycarbonyl-1,2-dihydroquinoline)<sup>26</sup> in  $\text{CH}_3\text{CN}$  (entry 6), or *N*-methyl-2-chloropyridinium iodide/ $\text{Et}_3\text{N}$ <sup>27</sup> (entry 7) gave the product **6** in approx. 50% yield. Better results were obtained when the acid **3** was activated as *p*-nitrophenyl ester<sup>28</sup> (68%, entry 8), or when the reaction was performed in the presence of  $(\text{PyS})_2(2,2'$ -dipyridyldisulfide)/ $\text{PPh}_3$  (triphenylphosphine)<sup>29</sup> (78%, entry 9); but careful purification by column chromatography was necessary in both cases. However, excellent results were obtained when the acid function in **3** was activated as pentafluorophenyl ester<sup>30</sup> (87%, entry 10).

Thus, treatment of **3** with pentafluorophenyl trifluoroacetate/ $\text{Py}$  in DMF gave, in almost quantitative yield, the corresponding activated ester, which was immediately reacted with **5** with *i*- $\text{Pr}_2\text{EtN}$  in dry DMF at room temperature overnight. A single crystallisation of the crude reaction mixture gave the bis-acetylated product **6** in 77% yield, which was used without any further purification. Additional product (10%) was isolated from the residue by column chromatography.

Subsequent removal of the protecting benzyl group by catalytic hydrogenolysis was achieved under pressure (3 atm) and acid conditions ( $\text{Pd}(\text{OH})_2/\text{C}$ ,  $\text{CH}_3\text{COOH}$ ), or at atmospheric pressure in MeOH, in the presence of 10% Pd/C cat. The second method afforded the free ligand in almost quantitative yield as a whitish solid, which was purified as a white dihydrochloride salt. The desired ligand was obtained in 61% overall yield from the 2,3-dihydroxypyridine, and the methodology allows the preparation of the ligand in gram quantities.

Scheme 1 Synthesis of **L**.

Finally, following the report of Taylor *et al.*<sup>21</sup> concerning the activation of the carboxylic function in 1-carboxymethyl-3-hydroxy-2(1*H*)-pyridinone as phthalimidohydroxy ester and the coupling with *N,N,N*-triethylamine, we tried the same conditions for the direct preparation of **L**. In our case, only a negligible amount of the free ligand **L** was obtained using the *N*-benzohydroxysuccinimide/DCCI system, whereas a 13% yield was obtained when the carboxylic function was activated with pentafluorophenyl trifluoroacetate/Py.

### Description of the structure

[HL]Cl·8H<sub>2</sub>O: the asymmetric unit of [HL]Cl·8H<sub>2</sub>O contains a molecule of the monocharged ligand, a chloride ion and eight water molecules. The conformation of the [12]aneN<sub>4</sub> ring can be described by the sequence of its dihedral angles as [2424] C corners,<sup>31</sup> thus resulting that the nitrogen atoms N(3) and N(5) are closer to each other than are the N(2) and N(4) atoms (2.785(4) Å *vs.* 5.427(4) Å) (Fig. 1). The former couple interacts *via* hydrogen bonding: the acidic hydrogen atom is bound to N(3) (N(3)–H(N3) bond distance 1.19(7) Å) and only 1.64(8) Å far from N(5), the angle N(3)–H(N3)–N(5) is 158(6)°.

As expected the nitrogen atoms N(2) and N(4) have a sp<sup>2</sup> hybridization as provided by the sum of the values of the bond angles around them (both are *ca.* 360°).

The two pyridinone rings are in a plane with the amidic C=O bonds almost perpendicular to the mean plane and iso-oriented. This latter plane forms an angle of 79.4(1)° with the mean plane passing through the nitrogen atoms N(2), N(3), N(4) and N(5). The [12]aneN<sub>4</sub> ring and the oxygen atoms O(2) and O(5) of the pyridinone rings, define a parallelepiped shaped cavity within the ligand. Its dimensions could be delimited by the distances N(2)–N(4) (5.427 Å) and N(3)–N(5) (2.785 Å) concerning the base of the parallelepiped, while the height of the polyhedron has been calculated as the distance between the geometrical centroid of the base (involving the four nitrogen atoms) and the geometrical centroid of the oxygen atoms O(2) and O(5): its value is about 7 Å. In this region of space are located two water molecules O(10) and O(7) (Fig. 1). The first one is located in the center of the cavity delimited by the [12]aneN<sub>4</sub> ring and the O(1) and O(6) oxygen atoms: with respect to the geometrical centroid calculated with the above mentioned nitrogen atoms, this water molecule is shifted upward, towards the pyridinone rings, of 1.37 Å. O(10) interacts with the atoms O(1) and O(6) *via* hydrogen bonds, being the distances 2.809(5) and 2.907(5) Å, respectively. Concerning the water molecule O(7), it has been found that it is almost equidistant from the four oxygen atoms of the pyridinone rings (the mean distance is 3.055 Å) and lies above

their mean plane (the displacement is 0.866(4) Å) towards the O(8) water molecule, with which it forms an H-bond interaction (2.913 Å). The water molecule labeled as O(11) is outside the parallelepiped cavity and interacts with both O(1) and O(6) (being the distances 2.909(7) and 2.906(4) Å respectively): it lies behind the plane formed by the pyridinone oxygen atoms (the displacement is 1.888(5) Å), opposite to the O(10) atom. Finally the water molecule O(9) interacts with the carbonyl oxygen atom O(3) (2.774(4) Å). There are also two intermolecular contacts both involving the carbonyl atom O(5): it interacts with O(5) and O(7) of symmetry related molecules both of these reported by the operation  $-x, -y, -z + 2$ . The distances are respectively 3.070(6) and 2.726(5) Å. The oxygen atom O(4) doesn't take part in any H-bond interaction.

### Molecular modelling

The following relevant results (all the calculations were performed using a distance-dependent dielectric constant set to 80) were obtained:<sup>32</sup>

i) The ligand, both in the neutral (**L**) and in the monoprotonated (HL<sup>+</sup>) form, appears quite rigid: both the 12-membered ring and the side arms are characterized by stiffness.

The ligand in the neutral species prefers, quite surprisingly,<sup>33</sup> a [2424] C corner conformation<sup>31</sup> which is preserved in HL<sup>+</sup>. Geometry optimizations performed on different conformations of simplified models of **L** and HL<sup>+</sup> (1,7-dimethyl-4,10-diacetyl-1,4,7,10-tetraazacyclododecane in the neutral and mono-protonated forms) revealed that the stereochemistry of the two sp<sup>2</sup> nitrogen atoms could be the origin of the observed rectangular shape of the uncharged ring.<sup>34</sup>

Concerning the mobility of the side arms, inspections of MD trajectories showed that the two pyridinone rings are virtually facing each other throughout the simulations: the average angle between them being 60°, while about 6 Å separate their centroids.

ii) The energy profile concerning the reorientation of the amide bonds of HL<sup>+</sup> shows that the *cis* and the *trans* isomers (*cis* isomer has the carbonyl groups *iso*-oriented while the *trans* one has the CO moieties pointing in opposite directions) have almost the same energy content, thus they both appear to be likely in solution. The *cis* species having the two C→O vectors pointing in the same direction with respect to the N→H one (which is almost identical to the X-ray structure) is slightly destabilized by about 1.6 kcal mol<sup>-1</sup>. The height of the barrier to be overcome for the *trans*→*cis* interconversion is about 16 kcal mol<sup>-1</sup>.

In summary, the dynamic behavior of HL<sup>+</sup> (as well as **L**) shows a relative 3D arrangement which produces a high number of preorganised bonding sites meeting just outside the cavity of the ligand, thus indicating that the ligand could

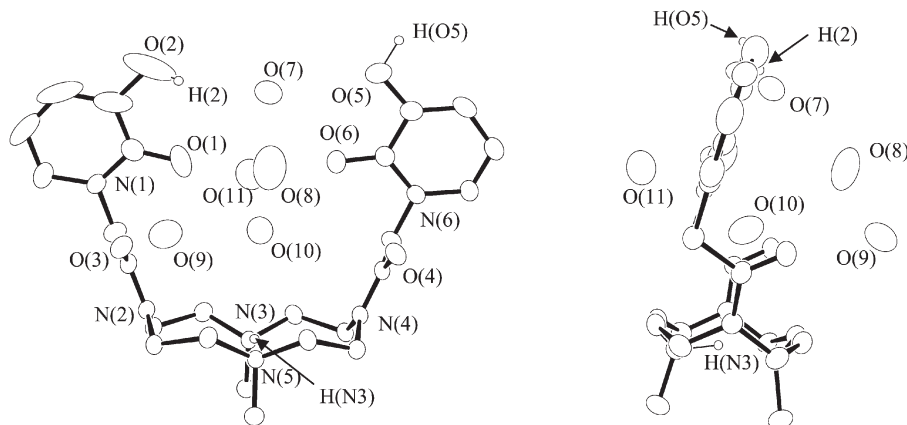


Fig. 1 Front and side view of HL<sup>+</sup> cation with five coordinated water molecules.

bind small charged species such as metal ions or polyatomic cations near the molecular surface.

To verify the latter hypothesis, the complexation properties of  $\text{HL}^+$  with respect to different  $\text{HG}^+$  species (*i.e.*  $\text{HG}^+ = \text{NH}_4^+$ ,  $\text{MeNH}_3^+$ ,  $\text{Me}_2\text{NH}_2^+$  and  $\text{Me}_3\text{NH}^+$ ) were tested by means of MD simulations.<sup>35</sup>

The results obtained are summarized below:

i)  $\text{HL}^+$  interacts with the complex cations  $\text{NH}_4^+$  and  $\text{MeNH}_3^+$ , whereas no stable adducts are formed with  $\text{Me}_2\text{NH}_2^+$  and  $\text{Me}_3\text{NH}^+$ , thus implying that at least three intermolecular hydrogen bonds are essential to stabilize the  $\text{HL}^+/\text{HG}^+$  complex. Stable  $\text{HL}^+/\text{HG}^+$  adducts show all the six oxygen atoms of the ligand cooperating in the substrate binding.

It is noteworthy that the overall shape of  $\text{HL}^+$  does not change significantly upon complexation with  $\text{HG}^+$  and that it closely resembles that found in the above reported MD results<sup>32</sup> (whose calculations were performed in mimicked aqueous solution using a distance dependent dielectric constant). This implies that the use of  $\epsilon = 1$  is, in this case, somewhat justified.

ii) There is no doubt that the pyridinone moieties play a key role in stabilizing the adducts, in particular the  $-\text{OH}$  functional groupings. In fact, substitution of both the  $-\text{OH}$  binding sites of the ligand with species unable to form H-bonds leads to the lack of formation of any adducts. Particularly, MD simulations showed that at least one hydroxyl group is essential for the adduct stabilization. In contrast, the presence of the amide oxygen atoms does not seem crucial in influencing the complexation behaviour of the ligand.

## Solution studies

**Basicity.** Table 2 summarizes the basicity constants of **L** as determined potentiometrically in  $0.15 \text{ mol dm}^{-3} \text{ NMe}_4\text{Cl}$  aqueous solution at 298.1 K. The neutral compound **L** behaves as a diprotic base and as diprotic acid under the experimental conditions used. As shown in Table 2, **L** can be present in solution as anionic species  $\text{H}_{-2}\text{L}^{2-}$ , indicating the removal of the two acidic hydrogens of the pyridinone moieties; moreover, **L** can add two protons to form the  $\text{H}_2\text{L}^{2+}$  species. By analyzing the protonation constants starting from the anionic species, it was found that **L** behaves as a rather strong base in the first three protonation steps with protonation constant values ranging from 10.79 for  $\log K_1$  to 8.33 for  $\log K_3$ , while it showed a sharp decrease in the last step with  $\log K_4 = 1.86$ . This trend suggests an easy availability of protonation sites in the first three steps in agreement with the topology of the ligands, which is prevented in the fourth step. The value of the  $\log K_1$

**Table 2** Logarithm of the protonation constants of **L** and formation constants of **L** with the guests ( $\text{HG}^+$ )  $\text{NH}_4^+$ , and  $\text{MeNH}_3^+$  determined by means of potentiometric measurements in  $0.15 \text{ mol dm}^{-3} \text{ NMe}_4\text{Cl}$  aqueous solutions at 298.1 K

Reaction	$\log K$	
$\text{H}_{-2}\text{L}^{2-} + \text{H}^+ = \text{H}_{-1}\text{L}^-$	10.79(1) <sup>a</sup>	
$\text{H}_{-1}\text{L}^- + \text{H}^+ = \text{L}$	9.08(1)	
$\text{L} + \text{H}^+ = \text{HL}^+$	8.33(1)	
$\text{HL}^+ + \text{H}^+ = \text{H}_2\text{L}^{2+}$	1.86(2)	
Reaction	$\text{NH}_4^+$	$\text{CH}_3\text{NH}_3^+$
$\text{L} + \text{HG}^+ = \text{HLG}^+$	—	1.69(2)
$\text{HL}^+ + \text{HG}^+ = \text{H}_2\text{LG}^{2+}$	2.12(3)	2.05(4)
$\text{H}_2\text{L}^{2+} + \text{HG}^+ = \text{H}_3\text{LG}^{3+}$	3.25(4)	2.89(3)

<sup>a</sup> Values in parentheses are the standard deviations on the last significant figure.

is similar to that found for the free tetraaza-macrocyclic base ( $\log K_1 = 10.76$ ),<sup>17</sup> suggesting an involvement of the amine functions in the stabilization of the first proton. Considering the disposition of the four protonable sites located far from each other, the low value of the fourth protonation constant suggests that the remaining protonable site in the  $\text{HL}^+$  species must be strongly involved in a H-bond network, thus limiting its availability.

UV-VIS absorption electronic spectra of **L** in aqueous solutions recorded at different pH values gave further information about the role of the pyridinone moieties in the acid–base behavior of **L**. The spectra show different features in acid or basic pH fields; at  $\text{pH} = 2$ , where the  $\text{H}_2\text{L}^{2+}$  species is prevalent in solution (Fig. 2), two  $\lambda_{\text{max}}$  at 236 ( $\epsilon = 9200 \text{ cm}^{-1}\text{mol}^{-1}\text{dm}^3$ ) and 299 nm ( $\epsilon = 13900 \text{ cm}^{-1}\text{mol}^{-1}\text{dm}^3$ ) can be observed, while at pH higher than 7.0 two new bands with  $\lambda_{\text{max}}$  at 254 and 312 nm appear, reaching their maximum absorbance values at  $\text{pH} = 10$  ( $\epsilon_{254} = 10500 \text{ cm}^{-1}\text{mol}^{-1}\text{dm}^3$ ,  $\epsilon_{312} = 16500 \text{ cm}^{-1}\text{mol}^{-1}\text{dm}^3$ ); no further changes were observed in the spectra at more strongly alkaline pH. These different spectral features can be ascribed to the presence in solution of the neutral form of the pyridinone moieties at low pH values and to their deprotonated form at alkaline pH values.<sup>15c</sup> In monitoring the spectra from acidic to basic pH, the appearance of the new bands at 254 and 312 nm, due to the pyridinonate moiety, was found to occur at pH over 7.0, where the **L** species starts to exist in solution, reaching its maximum values in absorbance at  $\text{pH} = 10$  where the  $\text{H}_{-1}\text{L}^-$  species has fully formed, thus proving that the deprotonation of the pyridinones occurs in the **L** and in the  $\text{H}_{-1}\text{L}^-$  species. Finally, the last deprotonation step, in which the  $\text{H}_{-2}\text{L}^{2-}$  species is formed, must involve the amine base, taking into account that the spectral feature does not change at pH values above 10 where such species start to form.

**<sup>13</sup>C and <sup>1</sup>H NMR study of **L**.** In order to obtain further structural information about the protonated species, <sup>1</sup>H and <sup>13</sup>C NMR spectra were recorded in the pH range of the potentiometric measurements. The <sup>13</sup>C NMR spectrum recorded at pH 12 and 298 K where the dianionic species  $\text{H}_{-2}\text{L}^{2-}$  is prevalent in solution, exhibits twelve resonances in the aliphatic range and six at higher ppm values (Fig. 3). Moreover, the <sup>1</sup>H NMR spectrum recorded at the same temperature and pH shows three singlets at 2.18, 2.23 and 2.28 having an integration ratio of 1 : 2 : 1, respectively, attributed to the N–CH<sub>3</sub> resonances (see Fig. 6). The presence of three signals for the two methyl groups of **L**, together with the number of aliphatic resonances in the <sup>13</sup>C NMR spectrum, suggests the existence of two conformers in solution called  $\text{H}_{-2}\text{L}_a^{2-}$  and  $\text{H}_{-2}\text{L}_b^{2-}$  which slowly interchange on the NMR time scale. The conformers are produced by the rotational restriction of the amide

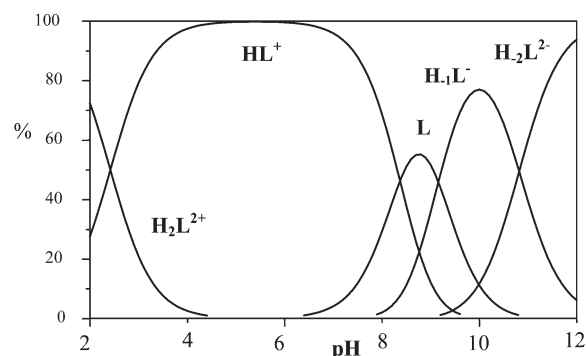


**Fig. 2** Distribution diagram of the species of **L** as a function of pH, in aqueous solution at  $298.1 \pm 0.1 \text{ K}$ , in  $0.15 \text{ mol dm}^{-3} \text{ NMe}_4\text{Cl}$ .

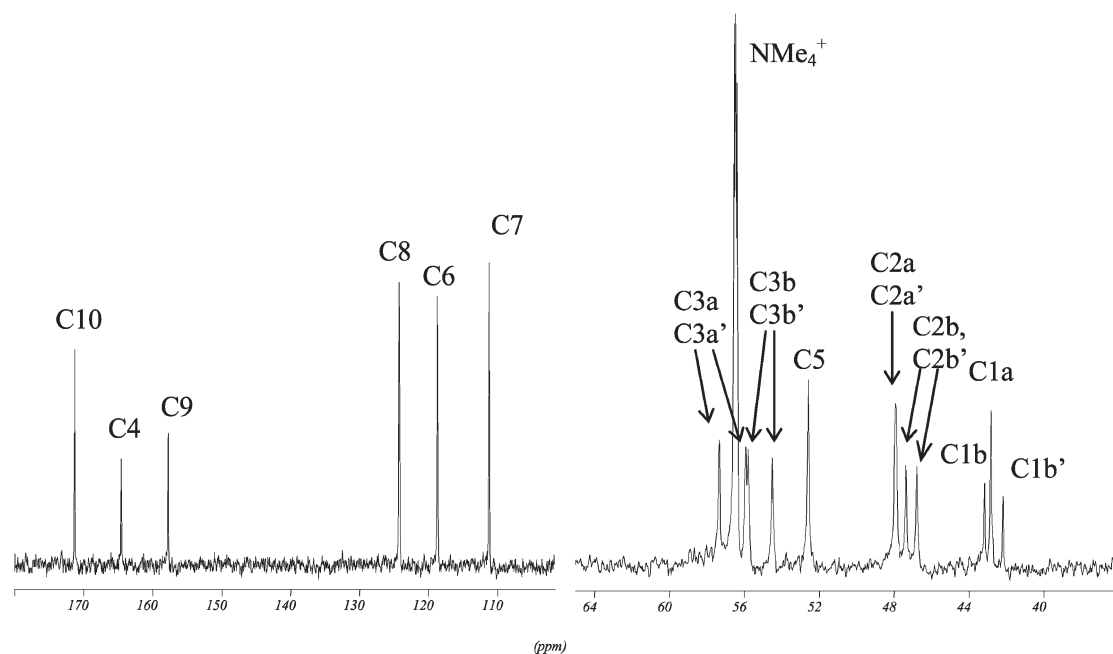


Fig. 3  $^{13}\text{C}$  NMR spectrum of the  $\text{H}_{-2}\text{L}^{2-}$  species, recorded in aqueous solution at  $\text{pH} = 12$ .

groups of the tetraaza-base, as previously revealed by MM studies. The side arms show the same frequency for both conformers, indicating that they are not affected by rotational restriction. The conformer  $\text{H}_{-2}\text{L}_a^{2-}$ , showing one singlet for the two methyl groups in both  $^1\text{H}$  and  $^{13}\text{C}$  NMR spectra, and four signals for the carbon atoms of the ethylene chains, denotes a  $\text{C}_2$  symmetry. The conformer  $\text{H}_{-2}\text{L}_b^{2-}$ , showing again four signals for the carbon atoms of the ethylene chains, but two signals for the methyl groups, both in  $^1\text{H}$  and  $^{13}\text{C}$  NMR spectra, has a  $\text{C}_s$  symmetry mediated on the NMR time scale. In substance, the two carbonyl groups can be *iso*-oriented (*cis*) in  $\text{H}_{-2}\text{L}_b^{2-}$  or pointing in the opposite direction (*trans*) in  $\text{H}_{-2}\text{L}_a^{2-}$  with respect to a plane passing through the two amide nitrogen atoms of the macrocyclic base (see Fig. 4). The calculated relative percentage of the two conformers is 1 : 1 at 298 K for the  $\text{H}_{-2}\text{L}^{2-}$  species, but it changes by lowering the pH. The relative percentage of the *cis* conformer is 59% at  $\text{pH} 10$ , where the  $\text{H}_{-1}\text{L}^-$  species is prevalent in solution (see Fig. 2), 62% at  $\text{pH} 8.4$ , 69% at  $\text{pH} 5$  where the  $\text{HL}^+$  species is prevalent, and 69% at  $\text{pH} 2$ . This means that the *cis*-orientation of the carbonyl groups, in agreement with the solid state structure, is preferred with respect to the *trans*-one when protonation occurs in the ligand.

The chemical shifts due to the same atoms of the different conformers undergo approximately the same shift when the pH is changed. This result suggests that the location of the acidic protons in the protonated species is substantially the same in both conformers. The trends in chemical shifts of the positively identified and significant  $^1\text{H}$  and  $^{13}\text{C}$  NMR

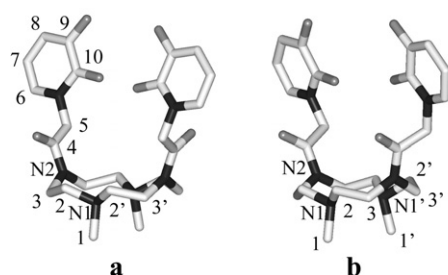


Fig. 4 Proposed models for the *cis* and *trans* conformers of **L**, together with labels for the NMR resonances.

resonances are reported in Fig. 5a and 5b, respectively, as a function of pH.

As shown in Fig. 5a, starting from  $\text{pH} 12$  to  $\text{pH} 10$  where the species  $\text{HL}^-$  is prevalent, the resonances of the methyl protons H1a, H1b, H1b', reveal a marked downfield shift, indicating that protonation takes place on the amine-methyl functions

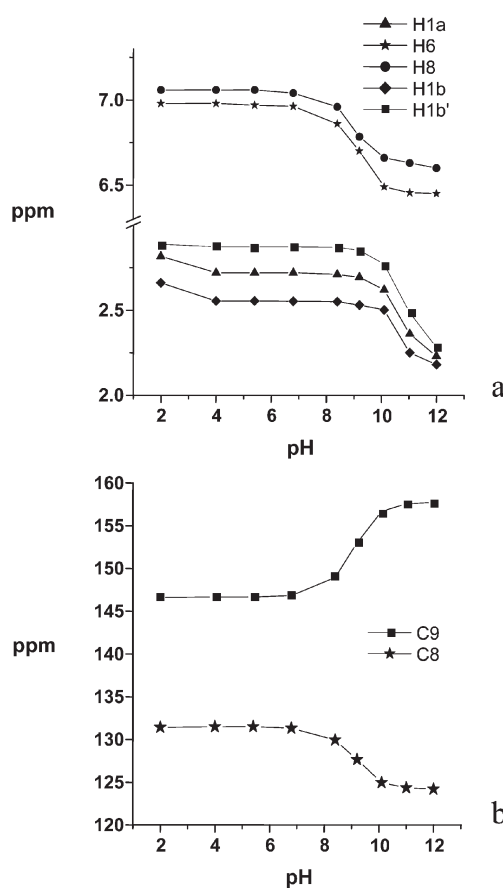
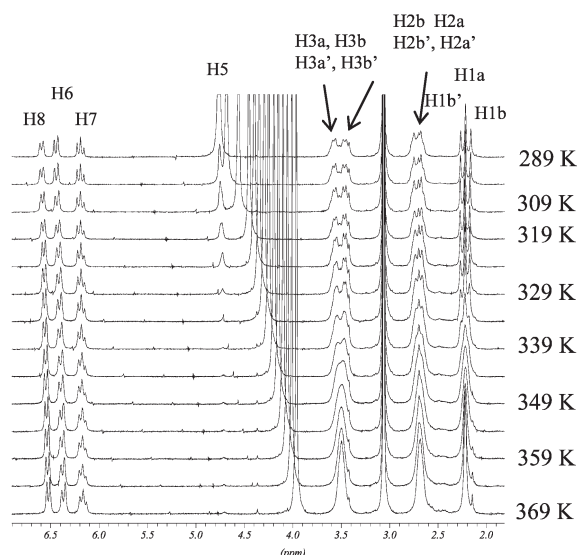


Fig. 5 Experimental NMR chemical shifts of **L** in aqueous solution, as a function of pH.  $^1\text{H}$  NMR (a);  $^{13}\text{C}$  NMR (b). Only the signals clearly attributed and showing significant shifts are reported.

of the macrocyclic base in both conformers. This hypothesis is in agreement with the results of the UV experiments (see above) and with the  $^{13}\text{C}$  NMR resonances, which do not show any shift for the signals due to the pyridinone groups (Fig. 5b). Moreover, H1b' undergoes a more marked shift than H1b, suggesting that the nitrogen atom N1' is more involved than N1 in the protonation of the *cis*-conformer. In the pH range 9–4, where the L and above all the  $\text{HL}^+$  species exists in solution, the signals of H6 and H8 undergo a downfield shift, indicating an increase in the positive charge on the pyridinone groups (Fig. 5a). These features indicate that the second and third protonation steps, in agreement with the UV experiments, involve the pyridinone groups on the oxygen atoms bound to C9. This hypothesis is in agreement with the downfield and upfield shifts of the C8 and C9 signals, respectively, in the  $^{13}\text{C}$  NMR spectra in the same pH range (Fig. 5b). The fourth protonation step, to obtain the  $\text{H}_2\text{L}^{2+}$  species, occurs below pH 3 and mainly causes a downfield shift of protons H1a and H1b in the  $^1\text{H}$  NMR spectra, suggesting that protonation takes place on the tertiary amine groups and, in the case of the *cis*-conformer, mainly involves the nitrogen atom N1.

**Dynamic variable-temperature NMR analysis.** Variable-temperature  $^1\text{H}$  NMR spectra of  $\text{H}_2\text{L}^{2-}$  species recorded in  $\text{D}_2\text{O}$  at pH 12 in the temperature range 289–369 K show the exchange process characteristic of the rotational restriction of the amide groups (Fig. 6). At high temperatures, the three sharp signals due to the N– $\text{CH}_3$  resonances observed at room temperature reveal a slow intermediate exchange, achieving a completely free interconversion for the equilibrium  $\text{H}_2\text{L}_a^{2-} = \text{H}_2\text{L}_b^{2-}$  up to 355 K. The rate constants at different temperatures were calculated using the gNMR 4.0 program<sup>36</sup> by varying their values until satisfactory fits between simulated and experimental data were obtained. From the values of the rate constants at different temperatures and applying the Eyring-plot method, a straight line was obtained from which the activation parameters were derived.

The calculated activation terms are:  $\Delta H^\ddagger = 12.7 \text{ kcal mol}^{-1}$ ,  $\Delta S^\ddagger = -14.8 \text{ cal mol}^{-1} \text{ K}^{-1}$ ,  $\Delta G^\ddagger = 17.1 \text{ kcal mol}^{-1}$ , respectively. These values for the activation energies are in agreement with those reported in the literature for the free rotation of an amide group.<sup>37</sup> This means that the amide groups in the  $\text{H}_2\text{L}^{2-}$  species are independent and, above all, that the two side-arms do not interact with each other or with the macrocyclic base.



**Fig. 6**  $^1\text{H}$  NMR spectra of  $\text{H}_2\text{L}^{2-}$  species, recorded in aqueous solution at pH = 12, recorded at different temperatures.

The fast exchange limit for the protonated species was not fully observable, denoting that the dynamic process is slightly dependent on the protonation of the ligand. In fact, applying the same method at pH 5.5, where the  $\text{HL}^+$  species is prevalent in solution, we obtained approximately the same values of free energy but different calculated activation terms:  $\Delta H^\ddagger = 16.6 \text{ kcal mol}^{-1}$ ,  $\Delta S^\ddagger = -2.7 \text{ cal mol}^{-1} \text{ K}^{-1}$ ,  $\Delta G^\ddagger = 17.4 \text{ kcal mol}^{-1}$ , respectively. The higher value of enthalpy for  $\text{HL}^+$  with respect to  $\text{H}_2\text{L}^{2-}$  species could explain why free rotation was not achieved in aqueous solution for the  $\text{HL}^+$  species. These experimental data can be ascribed to multiple factors including the formation of several H-bond contacts in the  $\text{HL}^+$  species also involving water molecules (see crystal structure), which slightly increase the activation enthalpy for the free rotation in this species.

**Binding of ammonium cations.** A good ligand for binding an ammonium guest in aqueous solution must have many preorganized hydrogen bonding sites. In this way, it can furnish multiple interactions with the guest to compensate the loss of solvation energy of ammonium. The preorganization of side-arms of L, which produces a high number of hydrogen bonding sites converging in a small area, as revealed by the molecular structure and suggested by MD simulations, induced us to explore the binding capability of the ligand towards simple organic charged cations.

The cations studied are the series of ammonium guests derived by ammonia, tertiary, secondary and primary methyl amines ( $\text{HG}^+$ ):  $\text{NH}_4^+$ ,  $\text{MeNH}_3^+$ ,  $\text{Me}_2\text{NH}_2^+$ , and  $\text{Me}_3\text{NH}^+$ . The L/G systems were potentiometrically studied in  $0.15 \text{ mol dm}^{-3}$   $\text{NMe}_4\text{Cl}$  aqueous solutions, at 298.1 K, using different L/G molar ratios. The protonation constants of the amines (G) were determined under our conditions and are substantially in agreement with those reported in the literature. For the  $\text{G} + \text{H}^+ = \text{HG}^+$  reaction,  $\log K = 9.24, 10.68, 10.81,$  and  $9.74$  for  $\text{G} = \text{NH}_3, \text{MeNH}_2, \text{Me}_2\text{NH},$  and  $\text{Me}_3\text{N}$ , respectively.

At first glance, by examining our results for the interactions of  $\text{HG}^+$  guests with the species of L, quantitatively reported in Table 2 as addition constants, it is possible to observe that, while  $\text{NH}_4^+$  and  $\text{CH}_3\text{NH}_3^+$  form stable adducts with some protonated species of L, no interactions were revealed for  $\text{Me}_2\text{NH}_2^+$ , and  $\text{Me}_3\text{NH}^+$  under our experimental conditions.

These results can be explained taking into account that dialkyl and trialkyl ammonium show lesser hydrogen bonding links than monoalkyl-ammonium or ammonium cations; this aspect influences not only the number of hydrogen bond contacts but also the statistical effect in the formations of such contacts, which is again favourable for the last two guests. However, the thermodynamic terms related to desolvation of host and guest and successive solvation of the adducts formed should be taken into account.

$\text{NH}_4^+$  and  $\text{MeNH}_3^+$  interact with  $\text{HL}^+$  and  $\text{H}_2\text{L}^{2+}$  species, while  $\text{MeNH}_3^+$  interact also with the neutral species L. This is attributed to the lower basicity of  $\text{NH}_3$ ; in fact,  $\text{NH}_4^+$  coexists in solution only with the  $\text{HL}^+$  and  $\text{H}_2\text{L}^{2+}$  species. Both guests show similar interaction with the same species of L however, they have a better interaction with the more highly charged  $\text{H}_2\text{L}^{2+}$  species. This further aspect confirms that the binding area of L is formed by the oxygen atoms of the preorganized side-arms, converging in an area of small dimension located far from the macrocyclic base in which the positive charges are localized. In this way, the base acts as a scaffold to preorganize the side-arms, allowing the interaction with these guests in aqueous solution.

## Conclusions

The synthesis of a new ligand containing two pyridinone side-arms attached on a tetraaza macrocyclic scaffold is reported.

Different synthetic routes for attaching side-arms were explored and it has been found that the pentafluorophenyl ester gave the best results.

The neutral species **L** behaves as diprotic base and as diprotic acid in aqueous solution under the experimental conditions used. Two conformers of **L** exist in solution on the NMR time scale, showing a *trans*- or a *cis*-orientation of the two carbonyl groups linked to the macrocyclic base. The activation parameters for the free interconversion of the two conformers in aqueous solution were calculated. The relative ratios of the two conformers are 1:1 in the  $H_2L^{2-}$  species while, in the protonated species, the *cis*-conformer prevails over the *trans*-, reaching a 2:1 molar ratio in the  $HL^+$  species. The NMR experiments underlined, in agreement with the UV spectra, that the first protonation step takes place on the amine functions of the macrocyclic base, while the pyridinone moieties are involved only in the second and third steps.

Conformational studies performed by molecular modelling showed that transformation of the two secondary amine functions of the tetraaza-macrocyclic base in the amide groups stiffened the molecular skeleton. Moreover, the two N=C=O groups force the two 3-hydroxypyridinones to stay in the same part of the macrocycle ring with the oxygen atoms face to face; thus, the whole molecule appears to be preorganized for interaction with other species.

The crystal structure reveals that the  $HL^+$  species interacts with several water molecules *via* hydrogen bond contacts provided by the side-arms, suggesting that **L** could be a good receptor for small substrates having high affinity towards oxygen atoms. In fact, solution and MM studies indicate that protonated species of **L** can host ammonium guests. Such protonated species can discriminate between  $NH_4^+$  or  $MeNH_3^+$  and  $Me_2NH_2^+$  or  $Me_3NH^+$ , interacting only with the first two species but not with the third and the fourth.

In conclusion, the tetraaza-macrocyclic base acts as a scaffold to preorganize the side-arms, which form an electron rich area able to stabilize guests such the ammonium cation *via* hydrogen-bond interactions. Because **L** interacts also with methyl ammonium or water molecules, it could also act as host of amino acids and poly(alcohol)s, making it an attractive ligand for molecular recognition studies.

## Experimental section

### General methods

UV absorption spectra were recorded at 298 K on a Varian Cary-100 spectrophotometer equipped with a temperature control unit. IR spectra were recorded on a Shimadzu FTIR-8300 spectrometer. Melting points were determined on a Büchi melting point B 540 apparatus and are uncorrected. EI-MS spectra (70 eV) were recorded with a Fisons Trio 1000 spectrometer; ESI mass spectra were recorded on a ThermoQuest LCQ Duo LC/MS/MS spectrometer.

### Synthesis

All chemicals were purchased from Aldrich, Fluka and Lancaster in the highest quality commercially available. All the solvents were dried prior to use. Chromatographic separations were performed on silica gel columns by flash chromatography (Kieselgel 60, 0.040–0.063 mm, Merck). TLC analyses were performed on precoated silica gel on aluminium sheets (Kieselgel 60 F<sub>254</sub>, Merck). Ligand **L** was obtained following the synthetic procedure reported in Scheme 1. 1,4,7,10-tetraazacyclo-dodecane **5** was prepared as previously described.<sup>19</sup>

**3-(Benzyloxy)-1-(carboxymethyl)-2(1H)-pyridinone (3).** 2,3-Dihydroxypyridine **1** (10.3 g, 0.093 mol) and ethyl bromoacetate (51.5 mL, 0.465 mol) were mixed together and refluxed

under nitrogen for 48 h. Work up as described<sup>20</sup> gave the 1-[(ethoxycarbonyl)methyl]-3-hydroxy-2(1H)-pyridinone **2** (13.79 g, 0.07 mol) as colorless needle-like crystals; mp 150–152 °C [Lit.<sup>20</sup> mp 150–151]; MS (EI) *m/z* 197 ( $M^+$ , 100%), 151 ( $M^+ - OEt$ , 25%), 124 ( $M^+ - COOEt$ , 42%), 95 (42%), 68 (68%). <sup>1</sup>H NMR and <sup>13</sup>C NMR as reported.<sup>21</sup>

A solution of aq. NaOH 4M (20 mL, 0.08 mol) was added to a solution of the above pyridinone (13.79 g, 0.07 mol) in methanol (300 mL) and the mixture was stirred for 30 min. After this time additional 4M NaOH was added to maintain the pH constant at 12, followed by the addition of benzyl chloride (28.3 mL, 0.245 mol). The mixture was refluxed for 5 h, followed by work up as reported,<sup>20</sup> to give **3** (17.22 g, 95%; overall yield based on **2**: 71%) as colorless needle-like crystals; mp 185–186 °C [Lit.<sup>20</sup> mp 185–185.5]; MS (EI) *m/z* 259 ( $M^+$ , 34%), 200 ( $M^+ - CH_2COOH$ , 49%), 91 (100%). <sup>1</sup>H NMR and <sup>13</sup>C NMR as reported.<sup>21</sup>

**4-(N), 10-(N)-bis[2-(3-benzyloxy-2-oxo-2H-pyridin-1-yl)acetamido]-1,7-dimethyl-1,4,7,10-tetraazacyclododecane (6).** To a well stirred solution of 3-(benzyloxy)-1-(carboxymethyl)-2(1H)-pyridinone (2 g, 0.0077 mol) in dry DMF (5 mL) at 0 °C was added pyridine (0.69 mL, 0.0085 mol) followed by pentafluorophenyl trifluoroacetate (1.66 mL, 0.01 mol). The reaction mixture was stirred for 1 hour at room temperature, diluted with AcOEt (300 mL) and washed with 0.1 N aqueous HCl (3 × 50 mL), 5% aqueous NaHCO<sub>3</sub> (3 × 50 mL) and brine (1 × 50 mL). The organic solution was dried over Na<sub>2</sub>SO<sub>4</sub> and concentrated under reduced pressure. The pentafluorophenyl ester **4** was obtained in quantitative yield (3.28 g), and was used without any further purification.

A solution of the above pentafluorophenyl ester **4** in dry DMF (5 mL) was added dropwise over 30 min at 0 °C to a stirred solution of 1,7-dimethyl-1,4,7,10-tetraazacyclododecane **5** (0.77 g, 0.00386 mol) and *i*-Pr<sub>2</sub>EtN (2.69 mL, 0.0155 mol) in dry DMF (2 mL). The reaction mixture was stirred for 12 h at room temperature. The organic yellow solution was concentrated under reduced pressure and the yellow oily residue was diluted in CHCl<sub>3</sub> and precipitated by the addition of Et<sub>2</sub>O to give **6** (2.03 g, 77%) as a colorless solid. The organic solution was concentrated under reduced pressure and the residue was purified by silica gel chromatography (CH<sub>2</sub>Cl<sub>2</sub> saturated with NH<sub>3</sub>/methanol 99:1) to give additional **6** (0.26 g, 10%; 87% overall yield); mp 105–106 °C dec; FTIR (film): 2957, 2924, 2850, 2792, 1652, 1601, 1455, 1252, 1064 cm<sup>-1</sup>; MS *m/z* (ESI): 705.3 ( $[M + Na]^+$ ), 683.3 ( $[M + 1]^+$ ); <sup>1</sup>H NMR: (CDCl<sub>3</sub>) δ 7.49–7.25 (10H, m), 7.17–6.95 (2H, m), 6.73–6.60 (2H, m), 6.10–5.97 (2H, m), 5.08 (4H, s), 4.90–4.75 (4H, m), 3.72–3.40 (8H, m), 3.00–2.58 (8H, m), 2.55–2.19 (6H, m); <sup>13</sup>C NMR: (CDCl<sub>3</sub>) δ 168.3, 167.4, 158.2, 148.5, 136.4, 131.0, 130.5, 128.5, 127.9, 127.4, 116.1, 115.7, 104.5, 104.4, 70.7, 58.0, 57.2, 56.4, 56.2, 50.0, 49.7, 48.2, 46.7, 43.5, 42.8, 41.7 ppm; Anal. for C<sub>38</sub>H<sub>46</sub>N<sub>6</sub>O<sub>6</sub> (682.35): Calcd C 66.84, H 6.79, N 12.31; Found C 66.8, H 6.8, N 12.3%.

**4-(N),10-(N)-bis[2-(3-hydroxy-2-oxo-2H-pyridin-1-yl)acetamido]-1,7-dimethyl-1,4,7,10-tetraazacyclododecane (L).** 10% Pd/C (0.2 g) was added to a solution of **6** (2 g, 0.0029 mol) in dry MeOH (40 mL), and the mixture was hydrogenated at 3 atm for 15 h at room temperature. After that time, the mixture was filtered over Celite and the solution was concentrated under reduced pressure, to give **L** (1.43 g, 97%) as a purple solid; mp. 120–121 °C dec; MS *m/z* (ESI): 525.3 ( $[M + Na]^+$ ), 503.3 ( $[M + 1]^+$ ); FTIR (film): 3509, 3406, 3005, 2959, 2924, 2850, 1652, 1583, 1552, 1497, 1467, 1274, 1239, 1006, 984 cm<sup>-1</sup>; <sup>1</sup>H NMR (DMSO-*d*<sub>6</sub>): δ 9.00 (2H, bs), 7.18–7.02 (2H, m), 6.83–6.68 (2H, m), 6.18–6.04 (2H, m), 5.00–4.62 (4H, m), 4.11–3.40 (8H, m), 3.40–2.70 (8H, m), 2.70–2.41 (6H, m). <sup>13</sup>C NMR (DMSO-*d*<sub>6</sub>): 167.6, 167.4, 157.9, 146.6,

129.7, 129.6, 115.3, 115.1, 104.8, 58.1, 57.8, 50.4, 50.3, 46.3, 46.1, 46.0, 45.8, 42.9, 42.5, 42.2 ppm.

**L** was dissolved in ethanol (95%) and treated with a solution of ethanol (95%)/37% hydrochloric acid 1:1 to give the dihydrated hydrochloride salt **L**·2HCl·2H<sub>2</sub>O in almost quantitative yield as a white solid; mp 209–210 °C dec.; FTIR (film): 3502, 3396, 3002, 2959, 2921, 2850, 1650, 1581, 1551, 1465, 1408, 1272, 1134, 1074, 751 cm<sup>-1</sup>; <sup>1</sup>H NMR: (D<sub>2</sub>O, pH = 3) δ 7.03 (2H, d, *J* = 6.5 Hz), 6.95 (2H, d, *J* = 7.2 Hz), 6.30 (2H, dd, *J* = 6.5, 7.2 Hz), 5.05–4.78 (4H, m), 4.03–3.52 (8H, m), 3.51–3.01 (8H, m), 3.00–2.44 (6H, m); <sup>13</sup>C NMR: (DMSO-*d*<sub>6</sub>) δ 167.7, 167.6, 157.8, 146.6, 129.7, 129.6, 115.4, 115.2, 104.9, 58.4, 57.9, 57.3, 50.5, 46.0, 42.8, 42.5, 42.3; Anal. for **L**·2HCl·2H<sub>2</sub>O, C<sub>24</sub>H<sub>40</sub>Cl<sub>2</sub>N<sub>6</sub>O<sub>8</sub> (611.52): Calcd C 47.14, H 6.59, N 13.74; Found C 47.1, H 6.7, N 13.6.

**[HL]Cl·8H<sub>2</sub>O**. **L**·2HCl·2H<sub>2</sub>O (61.1 mg, 0.1 mmol) was dissolved in H<sub>2</sub>O (10 mL) and the pH adjusted to 6 with NaOH 0.1 M. Colorless crystals suitable for X-ray analysis formed in a day (47 mg, 73%). Anal. for **[HL]Cl**·8H<sub>2</sub>O, C<sub>24</sub>H<sub>51</sub>ClN<sub>6</sub>O<sub>14</sub> (647.12): Calcd C 42.20, H 7.52, N 12.30; Found C 42.1, H 7.6, N 12.2%.

### X-ray crystallography

Crystallographic data for **[HL]Cl**·8H<sub>2</sub>O were collected on a Siemens P4 diffractometer using graphite-monochromated Cu-K<sub>α</sub> radiation ( $\lambda = 1.5418 \text{ \AA}$ ), *T* = 298 K. Intensities data were corrected for Lorentz and polarization effects. The structure was solved by direct methods using the SIR97 program<sup>38</sup> and refined by full-matrix least squares against *F*<sup>2</sup> using all data (SHELX97<sup>39</sup>). An absorption correction was applied with the program DIFABS<sup>40</sup> once the structure was solved. Anisotropic thermal parameters were used for the non H-atoms. All the hydrogen atoms except H(O2), H(N3) and H(O5) were introduced in calculated positions with their temperature factors refined according to the corresponding values of their bound atoms. The atoms H(N3) and H(O5) were found in the difference Fourier map and refined isotropically, while a different strategy was adopted for H(O2). The latter atom was found in the  $\Delta F$  map, but its refinement was difficult, perhaps because the linked oxygen atom O(2) has a quite high temperature factor. As a consequence the position of the H(O2) atom was refined according to the bound oxygen atom as well as its temperature factor. The hydrogen atoms on the water molecules could not be located in the  $\Delta F$  map.

Geometrical calculations were performed using PARST97<sup>41</sup> and molecular plots were produced with the ORTEP3 program.<sup>42</sup> Table 3 reports details on the crystal data, data collection, structure solution and refinement for **[HL]Cl**·8H<sub>2</sub>O. CCDC reference number 213787. See <http://www.rsc.org/suppdata/nj/b3/b306778e/> for crystallographic data in .cif or other electronic format.

### Molecular modelling

The software used was InsightII version 98.0<sup>43</sup> provided by MSI and implemented on an IBM RISC/6000 3AT computer. The CVFF force field was used in all the molecular modeling calculations.

Several modeling strategies were set up in order to enlighten the conformational features of **L** and **HL**<sup>+</sup>.

Geometry optimizations were carried out on **L** and **HL**<sup>+</sup> and on several *ad hoc* simplified models in order to assess the role played by the side arms and by the H-bond donor/acceptor groupings in determining the conformational properties and in stabilising the adducts with the complex cations (details available as electronic supplementary information†).

The energy profile for the amide bonds of **HL**<sup>+</sup> was studied by means of systematic conformational searches carried out by

**Table 3** Crystallographic data and refinement parameters for compound **L**

Empirical formula	[C <sub>24</sub> H <sub>35</sub> N <sub>6</sub> O <sub>6</sub> ] <sup>+</sup> (Cl <sup>-</sup> ) 8(H <sub>2</sub> O)
Formula weight	682.15
Temperature (K)	298
Wavelength (Å)	1.54184
Crystal system	triclinic
Space group	P $\bar{1}$
<i>a</i> , <i>b</i> , <i>c</i> (Å)	9.506(4), 9.904(3), 20.616(6)
$\alpha$ , $\beta$ , $\gamma$ (°)	95.45(4), 98.14(4), 118.46(3)
Volume (Å <sup>3</sup> )	1659(1)
<i>Z</i> , <i>D</i> <sub>c</sub> (Mg m <sup>-3</sup> )	2, 1.365
$\mu$ (mm <sup>-1</sup> )	1.654
<i>F</i> (000)	730
Crystal size (mm)	0.4 × 0.4 × 0.6
$\theta$ range (°)	2.20 to 60.00
Reflections collected/unique	5850/4826
Data/restraints/parameters	4082/0/416
Goodness of Fit on <i>F</i> <sup>2</sup>	1.045
Final <i>R</i> indices [ <i>I</i> > 2 $\sigma$ ( <i>I</i> )]	<i>R</i> 1 = 0.0691, <i>wR</i> 2 = 0.1972
<i>R</i> indices (all data)	<i>R</i> 1 = 0.0782, <i>wR</i> 2 = 0.2090

rotating the amidic bonds  $\phi_1$  (C17–N2–C7–O3) and  $\phi_2$  (C12–N4–C18–O4, labels refer to the X-ray structure numbering scheme) in constant steps of 30° (range 0–360°). The resulting 144 conformations were minimized applying an external torque about the dihedral angles  $\phi_1$  and  $\phi_2$ . The conformers, as well as the energy barriers associated with their mutual interconversion, were found with the help of the UTN program.<sup>44</sup>

MD calculations were performed at 300 K and the Verlet leapfrog algorithm, with a time step of 1 fs, was used. Before starting the MD procedures the initial species were optimized until the convergence criterion was met (< 0.01 kcal mol<sup>-1</sup>). For every MD run the system was allowed to equilibrate for 50 ps and then a 500 ps dynamic study was performed (snapshot conformations were saved every ps). Based on the results obtained in NMR investigations, the **HL**<sup>+</sup> *cis*-isomer was chosen for the **HL**<sup>+</sup>/**HG**<sup>+</sup> studies.

### EMF measurements

Equilibrium constants for protonation and complexation reactions with **L** were determined by pH-metric measurements (pH = -log [H<sup>+</sup>]) in 0.15 mol dm<sup>-3</sup> NMe<sub>4</sub>Cl at 298.1 ± 0.1 K, using the fully automatic equipment that has already been described; the EMF data were acquired with the PASAT computer program.<sup>45</sup> For the substrates investigated, their basicities were determined under our experimental conditions. The combined glass electrode was calibrated as a hydrogen concentration probe by titrating known amounts of HCl with CO<sub>2</sub>-free NMe<sub>4</sub>OH solutions and determining the equivalent point by Gran's method,<sup>46</sup> which gives the standard potential *E*<sup>o</sup> and the ionic product of water (p*K*<sub>w</sub> = 13.83(1) at 298.1 K in 0.15 mol dm<sup>-3</sup> NMe<sub>4</sub>Cl, *K*<sub>w</sub> = [H<sup>+</sup>][OH<sup>-</sup>]). At least three potentiometric titrations were performed for each system in the pH range 2–11, using different molar ratio of **G**/**L** ranging from 1:1 to 4:1. All titrations were treated either as single sets or as separate entities, for each system; no significant variations were found in the values of the determined constants. The HYPERQUAD computer program was used to process the potentiometric data.<sup>47</sup>

### NMR experiments

<sup>1</sup>H and <sup>13</sup>C NMR spectra were recorded on a Bruker AC-200 instrument, operating at 200.13 and 50.33 MHz, respectively, and equipped with a variable temperature controller. The

temperature of the NMR probe was calibrated using the 1,2-ethandiol as calibration sample. For the spectra recorded in D<sub>2</sub>O, the peak positions are reported with respect to HOD (4.75 ppm) for <sup>1</sup>H NMR spectra, while dioxane was used as reference standard in <sup>13</sup>C NMR spectra ( $\delta = 67.4$  ppm). For the spectra recorded in CDCl<sub>3</sub> and DMSO-d<sub>6</sub> the peak positions are reported with respect to TMS. <sup>1</sup>H-<sup>1</sup>H and <sup>1</sup>H-<sup>13</sup>C correlation experiments were performed to assign the signals. Chemical shifts ( $\delta$  scale) are reported in parts per million (ppm values) relative to the characteristic peak of the solvent; coupling constants ( $J$  values) are given in hertz (Hz).

NMR spectra simulation was performed using the computer program gNMR 4.0.<sup>36</sup> A satisfactory fit between the simulated and observed spectra was judged both by visual comparison and by a least-squares fit. The activation parameters  $\Delta G^\ddagger$ ,  $\Delta H^\ddagger$ , and  $\Delta S^\ddagger$  were derived from linear regression analysis of the Eyring plot.

## Acknowledgements

Financial support from the Italian Ministero dell'Università e della Ricerca (PRIN2002) and CRIST (Centro Interdipartimentale di Cristallografia Strutturale, University of Florence) which provided the X-ray equipment, are gratefully acknowledged.

## References

- (a) C. J. Pedersen, *J. Am. Chem. Soc.*, 1967, **89**, 7017; (b) D. J. Cram and J. M. Cram, *Science*, 1984, **183**, 4127; (c) J. -M. Lehn, *Angew. Chem., Int. Ed. Engl.*, 1988, **27**, 89; (d) R. M. Izatt, K. Pawlak and J. S. Bradshaw, *Chem. Rev.*, 1995, **95**, 2529.
- (a) L. -F. Lindoy, *The chemistry of macrocyclic ligand complexes*, Cambridge University Press, Cambridge, 1989; (b) J.-S. Bradshaw, *Aza-crown Macrocycles*, Wiley, New York, 1993; (c) P. Dietrich, P. Viout, J.-M. Lehn, *Macrocyclic Chemistry*, VCH, Weinheim, 1993.
- (a) N. V. Gerbeleu, V. B. Arion and J. Burgess, *Template synthesis of macrocyclic compounds*, Wiley-VCH, Weinheim, 1999; (b) D. Parker, *Macrocyclic synthesis: A practical approach*, Oxford University Press, 1996.
- G. W. Gokel, *Crown Ethers and Cryptands Monographs in Supramolecular Chemistry*, ed. J. F. Stoddart, The Royal Society of Chemistry, Cambridge, 1992.
- S. Patai, A. Rapport, E. Weber, *Crown Ethers and Analogs*, Wiley, New York, 1998.
- (a) Y. A. Zoltov, *Macrocyclic compounds in analytical chemistry*, Wiley-Interscience, New York, 1997; (b) M. Formica, V. Fusi, M. Micheloni, R. Pontellini and P. Romani, *Coord. Chem. Rev.*, 1999, **1**; (c) E. Bardazzi, M. Ciampolini, V. Fusi, M. Micheloni, N. Nardi, R. Pontellini and P. Romani, *J. Org. Chem.*, 1999, **64**, 1335; (d) P. Dapporto, M. Formica, V. Fusi, M. Micheloni, P. Paoli, R. Pontellini, P. Romani and P. Rossi, *Inorg. Chem.*, 2000, **39**, 4663.
- (a) E. Kimura, T. Gotoh, S. Aoki and M. Shiro, *Inorg. Chem.*, 2002, **41**, 3239; (b) C. Bazzicalupi, A. Bencini, E. Berni, A. Bianchi, V. Fedi, V. Fusi, C. Giorgi, P. Paoletti and V. Valtancoli, *Inorg. Chem.*, 1999, **38**, 4115; (c) V. Fusi, A. Llobet, J. Mahia, M. Micheloni, P. Paoli, X. Ribas and P. Rossi, *Eur. J. Inorg. Chem.*, 2002, **4**, 987.
- (a) L. Mandolini and R. Ungaro, *Calixarene in Action*, eds., Imperial College Press, London, England, 2000; (b) A. Bianchi, K. Bowman-James, E. Garcia-España, *Supramolecular Chemistry of Anions*, Wiley-VCH, New York, 1997.
- S. Mizukami, T. Nagano, Y. Urano, A. Odani and K. Kikuchi, *J. Am. Chem. Soc.*, 2002, **124**, 3920.
- (a) P. Dapporto, V. Fusi, M. Micheloni, P. Palma, P. Paoli and R. Pontellini, *Inorg. Chim. Acta*, 1998, **275-276**, 168; (b) C. Bazzicalupi, A. Bencini, A. Bianchi, V. Fedi, V. Fusi, C. Giorgi, P. Paoletti, L. Tei and B. Valtancoli, *J. Chem. Soc., Dalton Trans.*, 1999, 1101.
- G. Xue, J. S. Bradshaw, N. K. Dalley, P. B. Savage, K.E. Krakowiak, R. M. Izatt, L. Prodi, M. Montalti and N. Zaccaroni, *Tetrahedron*, 2001, **57**, 7623.
- G. Ambrosi, P. Dapporto, M. Formica, V. Fusi, L. Giorgi, M. Micheloni, P. Paoli, R. Pontellini and P. Rossi, *Chem. Eur. J.*, 2003, **9**, 800.
- (a) C. J. Sunderland, M. Botta, S. Aime and K. N. Raymond, *Inorg. Chem.*, 2001, **40**, 6746; (b) J. Xu, E. Radkov, M. Ziegler and K. N. Raymond, *Inorg. Chem.*, 2001, **39**, 4156.
- P. W. Durbin, B. Kullgren and K. N. Raymond, *Health Phys.*, 1997, **72**, 865.
- (a) J. Xu, B. Kullgren, P. W. Durbin and K. N. Raymond, *J. Med. Chem.*, 1995, **38**, 2606; (b) M. Meyer, J. R. Telford, S. M. Cohen, D. J. White, J. Xu and K. N. Raymond, *J. Am. Chem. Soc.*, 1997, **119**, 10093; (c) B. L. Rai, H. Khodr and R. C. Hider, *Tetrahedron*, 1999, **55**, 1129.
- (a) G. Xiao, D. Van der Helm, R. C. Hider and J. B. Porter, *J. Med. Chem.*, 1996, **100**, 2345; (b) A. Shanzer, J. Libman, S. Lifson and C. E. Felder, *J. Am. Chem. Soc.*, 1986, **108**, 7609.
- X. X. Zhang, J. S. Bradshaw and R. M. Izatt, *Chem. Rev.*, 1997, **97**, 3313.
- (a) C. C. and Young, *J. Chem. Educ.*, 1997, **74**, 177; (b) J. Chin, J. Oh, S. Y. Jon, S. H. Park, C. Walsdorff, B. Stranix, A. Ghousoub, S. J. Lee, H. J. Chung, S. Park and K. Kim, *J. Am. Chem. Soc.*, 2002, **124**, 5374; (c) M. S. Ghauri and J. S. Thomas, *Analyst*, 1994, **119**, 2323.
- M. Ciampolini, P. Dapporto, M. Micheloni, N. Nardi, P. Paoletti and F. Zanobini, *J. Chem. Soc., Dalton Trans.*, 1984, 1357.
- M. Streater, P. D. Taylor, R. C. Hider and J. Porter, *J. Med. Chem.*, 1990, **33**, 1749.
- R. C. Fox and P. D. Taylor, *Synth. Commun.*, 1998, **28**(9), 1563.
- J. C. Sheehan and G. P. Hess, *J. Am. Chem. Soc.*, 1955, **77**, 1067.
- (a) M. T. Leplawy, D. S. Jones, G. W. Kenner and R. C. Sheppard, *Tetrahedron*, 1960, **11**, 39; (b) L. L. Lai, E. Wang and B. J. Luh, *Synthesis*, 2001, 361.
- M. Kunishima, C. Kawaki, J. Morita, K. Terao, F. Iwasaki and S. Tani, *Tetrahedron*, 1999, **55**, 13 159.
- J. C. Sheehan, P. A. Cruickshank and G. L. Boshart, *J. Org. Chem.*, 1961, **26**, 2525.
- B. Belleau, R. Martel, G. Lacasse, M. Ménard, N. L. Weinberg and Y. G. Perron, *J. Am. Chem. Soc.*, 1968, **90**, 823.
- (a) T. Mukaiyama, M. Usui and K. Saigo, *Chem. Lett.*, 1976, 49; (b) E. Bald, K. Saigo and T. Mukaiyama, *Chem. Lett.*, 1975, 1163; (c) T. K. Jones, R. A. Reamer, R. Desmond and S. G. Mills, *J. Am. Chem. Soc.*, 1990, **112**, 2998.
- M. Bodanszky and V. Du Vigneaud, *J. Am. Chem. Soc.*, 1959, **81**, 5688.
- (a) T. Mukaiyama, R. Matsueda and M. Suzuki, *Tetrahedron Lett.*, 1970, **22**, 1901; (b) S. Kobayashi, T. Iimori, T. Izawa and M. Ohno, *J. Am. Chem. Soc.*, 1981, **103**, 2406.
- M. Green and J. Berman, *Tetrahedron Lett.*, 1990, **31**, 5851.
- I. Bernal, *Stereochemical and Stereophysical Behaviour of Macrocycles*, Elsevier, 1987.
- A more detailed explanation of the results obtained is summarized in the supplementary material†.
- F. H. Allen, O. Kennard and Cambridge Structural Database, *J. Chem. Soc., Perkin Trans. 2*, 1989, 1131.
- P. L. Anelli, L. Calabi, P. Dapporto, M. Murrù, L. Paleari, P. Paoli, F. Uggeri, S. Verona and M. Virtuali, *J. Chem. Soc., Perkin Trans. 1*, 1995, 2995.
- No ligand-substrate interaction was detected in media simulated by means of a distance dependent dielectric constant  $\epsilon > 1$ , because this latter greatly attenuates the charge interactions, that is why the MD simulations on the adducts were performed in vacuum.
- gNMR 4.0, Cherwell Science, Oxford.
- J. Clayden, *Synlett.*, 1998, 810.
- A. Altomare, G. L. Cascarano, C. Giacovazzo, A. Guagliardi, M. Burla, G. Polidori and M. Camalli, *J. Appl. Cryst.*, 1999, **32**, 115.
- G. M. Sheldrick, *SHELX 97*, University of Göttingen, Germany, 1997.
- N. Walker and D. D. Stuart, *Acta Crystallogr. Sect. A*, 1993, **39**, 158.
- M. Nardelli, *Comput. Chem.*, 1983, **7**, 95.
- L. J. Farrugia, *J. Appl. Cryst.*, 1997, **30**, 565.
- Biosym/MSI, 9685 Scranton Road, San Diego, CA 92121-3752, USA.
- G. Ciolli, P. Dapporto, A. Guerri, P. Paoli and P. Rossi, *The UTN Program: computing interconversion energy between conformers in acyclic molecules*, Firenze University Press, <http://epress.unifi.it> 2002.
- M. Fontanelli, M. Micheloni, *I Spanish-Italian Congr. Thermodynamics of Metal Complexes*, Peñíscola, June 3-6, 1990, University of Valencia Spain, 41.
- (a) G. Gran, *Analyst*, 1952, **77**, 661; (b) F. J. Rossotti and H. Rossotti, *J. Chem. Educ.*, 1965, **42**, 375.
- P. Gans, A. Sabatini and A. Vacca, *Talanta*, 1996, **43**, 1739.